

Deep Reinforcement Learning for Traveling Purchaser Problems

Haofeng Yuan^a, Rongping Zhu^a, Wanlu Yang^a, Shiji Song^{a,*}, Keyou You^a, Wei Fan^b,
C. L. Philip Chen^c

^a*Department of Automation & BNRist, Tsinghua University, Beijing 100084, China*

^b*AI Laboratory, Lenovo Research, Beijing 100193, China*

^c*School of Computer Science and Engineering, South China University of Technology, Guangzhou 510641, China*

Abstract

The traveling purchaser problem (TPP) is an important combinatorial optimization problem with broad applications. Due to the coupling between routing and purchasing, existing works on TPPs commonly address route construction and purchase planning simultaneously, which, however, leads to exact methods with high computational cost and heuristics with sophisticated design but limited performance. In sharp contrast, we propose a novel approach based on deep reinforcement learning (DRL), which addresses route construction and purchase planning *separately*, while evaluating and optimizing the solution from a *global* perspective. The key components of our approach include a bipartite graph representation for TPPs to capture the market-product relations, and a policy network that extracts information from the bipartite graph and uses it to sequentially construct the route. One significant benefit of our framework is that we can efficiently construct the route using the policy network, and once the route is determined, the associated purchasing plan can be easily derived through linear programming, while, leveraging DRL, we can train the policy network to optimize the global solution objective. Furthermore, by introducing a meta-learning strategy, the policy network can be trained stably on large-sized TPP instances, and generalize well across instances of varying sizes and distributions, even to much larger instances that are never seen during training. Experiments on various synthetic TPP instances and the TPPLIB benchmark demonstrate that our DRL-based approach can significantly outperform well-established TPP heuristics, reducing the optimality gap by 40%-90%, and also showing an advantage in runtime, especially on large-sized instances.

Keywords: Traveling purchaser problem, deep reinforcement learning, bipartite graph, policy network, meta-learning

*Corresponding author

Email addresses: yhf22@mails.tsinghua.edu.cn (Haofeng Yuan), zhurp19@mails.tsinghua.edu.cn (Rongping Zhu), yangwl21@mails.tsinghua.edu.cn (Wanlu Yang), shijis@mail.tsinghua.edu.cn (Shiji Song), youky@mail.tsinghua.edu.cn (Keyou You), fanwei2@lenovo.com (Wei Fan), philipchen@scut.edu.cn (C. L. Philip Chen)

Contents

1	Introduction	3
2	Problem Formulation	5
3	“Solve Separately, Learn Globally” Framework	6
3.1	Overview	7
3.2	MDP Formulation	7
4	Bipartite Graph Representation for TPPs	9
5	Policy Network	11
5.1	Policy Network Architecture	11
5.2	Basic Training Algorithm	16
6	Meta-learning Strategy	17
7	Experiments	19
7.1	Experimental Settings	19
7.2	Training Performance	20
7.3	Results on Synthetic Instances	21
7.4	Results on TPPLIB Benchmark Instances	23
7.5	Generalization Performance on Large-Sized Instances	24
8	Conclusion	24
	Acknowledgements	25
	References	25

1. Introduction

The traveling purchaser problem (TPP) is a well-known combinatorial optimization (CO) problem, which has broad real-world applications and received much attention from both researchers and practitioners in recent decades (Burstall, 1966; Goldberg et al., 2009; Angelelli et al., 2016; Palomo-Martínez and Salazar-Aguilar, 2019). In the TPP, given a list of products and their demand quantities, the purchaser aims to decide a route and an associated purchasing plan to meet the product demands by visiting a subset of markets, with the objective to minimize the sum of traveling and purchasing costs (Ramesh, 1981).

Unfortunately, TPPs are known to be strongly NP-hard (Laporte et al., 2003). In particular, the main challenge in solving TPPs stems from the inherent coupling between routing and purchasing: the routing decisions have to take both traveling and purchasing costs into consideration, while the choice of visited markets will, in turn, impact the purchasing decisions and associated cost. Thus, existing works typically need to deal with both routing and purchasing simultaneously (Manerba et al., 2017), which, however, imposes many limitations. On the one hand, exact methods such as branch-and-cut (Laporte et al., 2003; Riera-Ledesma and González, 2006) require joint optimization of routing and purchasing decisions, which generically leads to high computational cost, making them often intractable for realistically sized problem instances. For example, solving a medium-sized TPP instance with 100 markets and 50 products can take hours on a computer with a 2.3 GHz processor, and the computational time grows exponentially with the problem size (Riera-Ledesma, 2012). On the other hand, various heuristic methods, such as the Generalized Savings Heuristic (GSH) (Golden et al., 1981), the Tour Reduction Heuristic (TRH) (Ong, 1982), and the Commodity Adding Heuristic (CAH) (Pearn and Chien, 1998), have been proposed to produce high-quality solutions for TPPs within a reasonable time. Readers are referred to Manerba et al. (2017) for further details. However, these heuristics have to carefully balance the effect of each operation on the traveling cost and purchasing cost, and thus rely heavily on sophisticated design that requires substantial human expertise and domain knowledge. Moreover, these hand-crafted heuristics typically need to be tailored case-by-case, resulting in that they may only be effective on limited instances with specific characteristics, and lack the ability to generalize across different instance distributions. For example, CAH performs poorly if the purchasing cost dominates in the optimization objective, and GSH may yield poor solutions if a market sells most of the products but is located far from other markets (Pearn and Chien, 1998).

In this paper, we propose a novel approach based on deep reinforcement learning (DRL), which addresses the limitations of existing methods by decoupling the treatment of routing and purchasing decisions. The core idea of our approach can be summarized as “*solve separately, learn globally*”. We note that by leveraging the forward-thinking and global-optimizing mechanisms of DRL, we can break the complex task of solving TPPs into two *separate* stages: route construction and purchase planning, while learning a policy to guide the decision-making towards optimizing the *global* solution objective. Specifically, in the first stage, we use a policy network to sequentially construct the route, where at each decision step the policy network takes the problem instance and current partial route as input, and outputs an action distribution to determine the next market to visit. Then, once a complete route is constructed, we proceed to the second stage, where we derive the optimal purchasing plan for the visited markets through an easily solvable linear transportation problem. Note that in the first stage, we use the policy network only to decide the route, i.e., which markets to visit and the visited order, deferring the decisions on specific purchasing plan to the second stage. This separation decouples the routing decisions and purchasing decisions at the

operating level, such that each stage can be efficiently done during the solving process. Meanwhile, to bridge the optimization interdependence between routing and purchasing, we train the first-stage policy network to optimize the global solution objective, which is determined jointly by both stages. In other words, though the policy network is only used for route construction in the first stage, it is learned to construct a high-quality route that can not only have low traveling cost, but also be promising to lead to a low-cost purchasing plan in the subsequent second stage, thus to minimize the overall solution objective.

In fact, the idea of leveraging DRL for CO problems is not entirely new though (Lopes Silva et al., 2019; Bengio et al., 2021; Que et al., 2023; Fajemisin et al., 2024), particularly in routing problems such as the traveling salesman problem (TSP) (Vinyals et al., 2015; Bello et al., 2017; Zhang et al., 2023; Gao et al., 2024) and the vehicle routing problem (VRP) (Nazari et al., 2018; Zhang et al., 2020; Kalatzantonakis et al., 2023; Rodríguez-Esparza et al., 2024). However, these efforts typically rely on problem-specific properties and are limited to problems with simple structures, which cannot be readily extended to TPPs. Therefore, considering the double nature of TPPs and building on our solution framework, we first propose a novel bipartite graph representation for TPPs, where the markets and products are represented as two sets of nodes, with the supply information (e.g., the supply quantities and prices) encoded as edge features between the market and product nodes. In contrast to existing representations for routing problems (e.g., the complete or k -NN graphs (Kool et al., 2019; Fu et al., 2021)), our bipartite graph representation can naturally capture the relations between markets and products through message-passing along edges. Then, we design a policy network, which can effectively extract information from the bipartite graph and use it for route construction. Specifically, our policy network exploits the connecting structure of the bipartite graph, and leverages graph neural networks (GNNs) and multi-head attention (MHA) to aggregate information both across and within the two sets of nodes. This effectively facilitates the extraction of relational information of the markets and products, such as the spatial relations between markets and the potential substitutions and complementarities in product supply, which is important for constructing a high-quality route. Moreover, it is worth mentioning that our bipartite graph representation and policy network have another appealing property: they are size-agnostic such that a trained policy network can be flexibly adapted to TPP instances of varying sizes without the need for retraining or parameter adjustment.

In addition, despite our proposed framework and the key DRL components introduced above, how to efficiently learn a high-quality policy remains another challenge. Due to the huge state-action space, a randomly initialized policy network may suffer from inefficient exploration, which can result in slow convergence or even training collapse, particularly on large-sized instances. Different from the training techniques or tricks (Kwon et al., 2020; Kim et al., 2022) designed for specific problems (mainly TSP or VRP), we propose an effective and more generalizable training strategy based on meta-learning (Finn et al., 2017). The strategy trains an initialized policy network on a collection of small-sized instances, with the learning objective to achieve fast adaptation to large-sized instances at low fine-tuning cost. Furthermore, we observe that the initialized policy network can learn cross-distribution knowledge through meta-learning, such that it can effectively generalize across varied instance sizes and distributions, even achieving good zero-shot generalization performance to instances of much larger sizes that are never seen during training.

We empirically evaluate our DRL-based approach on two types of TPPs: the restricted TPP (R-TPP), where the supply quantities of available products at each market are limited, and the unrestricted TPP (U-TPP), which assumes unlimited supply quantities. We conduct extensive

experiments on various synthetic TPP instances and the TPPLIB benchmark (Riera-Ledesma, 2012). The results demonstrate that our DRL-based approach can produce near-optimal solutions with high computational efficiency, significantly outperforming well-established TPP heuristics in both solution quality and runtime. Notably, our approach achieves an average optimality gap consistently within 6% on each category of the TPPLIB benchmark in our experiment, yielding a reduction of 40%-90% compared to the baseline heuristics. In addition, we further confirm the zero-shot generalization ability of the learned policy on instances that are much larger (up to 300 markets and 300 products, the largest size in TPPLIB) than the training instances.

The remainder of this paper is organized as follows. In Section 2, we formally describe TPPs and introduce the mathematical formulation. Section 3 presents our “solve separately, learn globally” framework for solving TPPs. Section 4 introduces the bipartite graph representation for TPPs, and Section 5 presents the details of our policy network, followed by a description of the basic training algorithm. In Section 6, we propose a meta-learning strategy for efficiently training on large-sized problems and improving generalization. Section 7 provides the empirical evaluation and reports the results and analysis. Finally, conclusions are drawn in Section 8.

2. Problem Formulation

In the TPP, a purchaser needs to buy a set of products from a set of markets. Each product can only be purchased from certain markets, with potentially varying supply quantities and prices at different markets. The purchaser aims to decide a route that visits a subset of markets and an associated purchasing plan to meet all product demands, with the objective to minimize the sum of traveling and purchasing costs.

Mathematically, a TPP is defined on a complete directed graph $\mathcal{G} = (V, E)$, where $V = \{v_0\} \cup M$ is the set of nodes and $E = \{(i, j) : i, j \in V, i \neq j\}$ is the set of edges. Node v_0 denotes the depot and M denotes the set of markets. The problem considers a set K of products to purchase, where a demand d_k is specified for each product $k \in K$. Each product k is supplied in a subset of markets $M_k \subseteq M$, where at most q_{ik} units of product k can be purchased from market $i \in M_k$, at a price of p_{ik} . The traveling cost associated with each edge $(i, j) \in E$ is denoted by c_{ij} . The purchaser needs to determine a route on \mathcal{G} , i.e., a simple cycle $\pi = (v_0, v^1, v^2, \dots, v^T, v_0)$, $T \leq |M|$, which starts and ends at the depot and visits a subset of markets, and decide how much of each product to purchase at each market to satisfy the demands at minimum traveling and purchasing costs. Note that to guarantee the existence of a feasible purchasing plan with respect to the product demand, it is assumed that $0 < q_{ik} \leq d_k$ for each $k \in K$ and $i \in M_k$, and $\sum_{i \in M_k} q_{ik} \geq d_k$ for each $k \in K$. In the case of U-TPP, the first assumption becomes $q_{ik} = d_k$ for all $k \in K$ and $i \in M_k$, i.e., the supply quantities for the available products at each market are unlimited, and otherwise R-TPP.

The TPP can be formulated as a mixed integer linear programming (MILP) problem. Let y_i be a binary variable taking value 1 if market i is selected, and 0 otherwise. Let x_{ij} be a binary variable taking value 1 if edge (i, j) is traversed, and 0 otherwise. Let z_{ik} be a variable representing the quantity of product k purchased at market $i \in M_k$. For a subset of nodes $V' \subset V$, we define:

$$\begin{aligned}\delta^+(V') &:= \{(i, j) \in E : i \in V', j \notin V'\}, \\ \delta^-(V') &:= \{(i, j) \in E : i \notin V', j \in V'\}.\end{aligned}$$

Then, the TPP can be formulated as follows (Laporte et al., 2003):

$$\min \sum_{(i,j) \in E} c_{ij}x_{ij} + \sum_{k \in K} \sum_{i \in M_k} p_{ik}z_{ik} \quad (1)$$

$$\text{s.t.} \quad \sum_{i \in M_k} z_{ik} = d_k, \forall k \in K, \quad (2)$$

$$z_{ik} \leq q_{ik}y_i, \forall k \in K, i \in M_k, \quad (3)$$

$$\sum_{(i,j) \in \delta^+(\{h\})} x_{ij} = y_h, \forall h \in V, \quad (4)$$

$$\sum_{(i,j) \in \delta^-(\{h\})} x_{ij} = y_h, \forall h \in V, \quad (5)$$

$$\sum_{(i,j) \in \delta^-(M')} x_{ij} \geq y_h, \forall M' \subseteq M, h \in M', \quad (6)$$

$$x_{ij} \in \{0, 1\}, \forall (i, j) \in E, \quad (7)$$

$$y_i \in \{0, 1\}, \forall i \in V, \quad (8)$$

$$z_{ik} \geq 0, \forall k \in K, i \in M_k. \quad (9)$$

The objective function (1) aims at minimizing the sum of traveling and purchasing costs. Constraints (2) ensure that all demands must be satisfied. Constraints (3) limit the quantity of product k purchased at market i to the available supply quantity, and prevent any purchase at unvisited markets. Constraints (4)-(5) impose that for each visited market, exactly one edge must enter and leave the node, and constraints (6) prevent sub-tours. Constraints (7)-(9) impose integrality conditions and bounds on the decision variables.

The MILP formulation (1)-(9) is commonly employed in exact methods for TPPs (Manerba et al., 2017). However, the number of constraints is exponential in the number of markets and the number of variables is also significantly large, which can lead to a massive branch-and-bound tree with weak lower bounds in an MILP solver. The branch-and-cut algorithms, as introduced in Laporte et al. (2003) and Riera-Ledesma and González (2006), attempt to alleviate this issue by dynamically generating variables and separating constraints, thereby to reduce the tree size and accelerate solving. Nonetheless, the dynamic pricing and separation procedures are still computationally expensive, making it often unaffordable to solve the MILP exactly in practice, especially for large-sized TPP instances. In contrast, our DRL-based approach does not directly solve the MILP, but instead creates a bipartite graph representation (Section 4) based on its structure, which is further used as input to the policy network for route construction.

3. “Solve Separately, Learn Globally” Framework

We now introduce our “solve separately, learn globally” framework for TPPs. As aforementioned, prior works typically require to address routing and purchasing simultaneously (Manerba et al., 2017). In contrast, by leveraging DRL, we can decouple the routing decisions and purchasing decisions at the operating level, i.e., “solve separately”, while guiding the decision-making using a policy, which is learned to optimize the global solution objective, i.e., “learn globally”. This framework offers the potential for both high computational efficiency and high-quality solutions if the policy is well-trained.

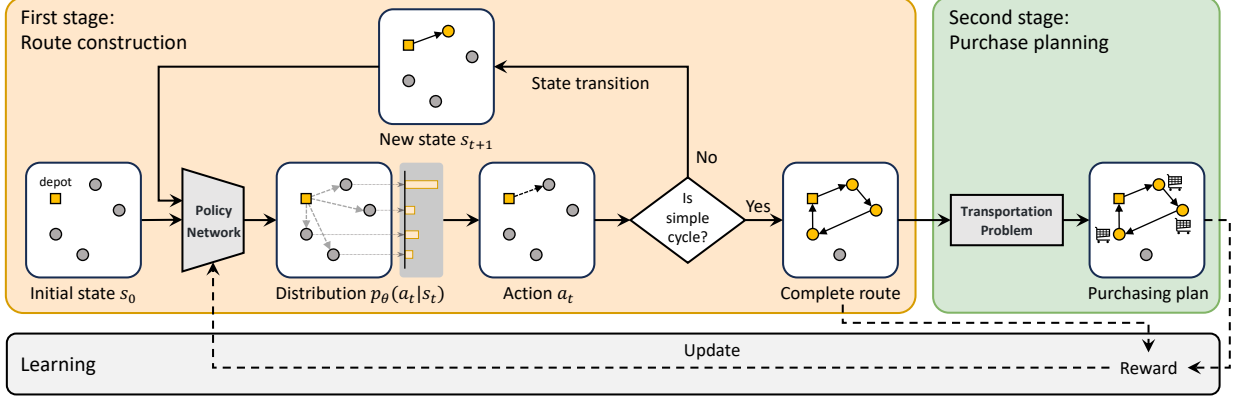


Figure 1: Our “solve separately, learn globally” framework. In the first stage, the purchaser starts from the depot, and selects a new node to add to the partial route based on a policy network at each decision step, until it returns to the depot and a complete route is made. Then in the second stage, the purchasing plan is derived through a transportation problem, which is integrated into the reward calculation procedure for the terminal state. The final reward is defined as the negative solution objective, which is used to update the policy network through a DRL training algorithm.

3.1. Overview

Figure 1 illustrates an overview of our proposed framework. The solving process consists of two separate stages: *route construction* and *purchase planning*. In implementation, we formulate this process as a Markov decision process (MDP), which provides a fundamental framework for DRL. Specifically, in the first stage, we sequentially construct the route through finite decision steps. The purchaser starts from the depot as the initial state, and at each decision step selects the next market (or the depot) to visit based on a policy, which is parameterized as a deep neural network (called the policy network). The route construction process iterates until the depot is revisited, i.e., a complete route is formed, and the MDP reaches the terminal state. Then, we proceed to the second stage, where we derive the optimal purchasing plan for the visited markets along the route by solving a linear transportation problem. In our implementation of MDP, the second stage is integrated into the reward calculation procedure for the terminal state. The final reward is defined as the negative solution objective, which is the sum of the traveling cost of the route constructed in the first stage and the purchasing cost derived in the second stage. The reward is then used to update the first-stage policy network through a DRL training algorithm.

3.2. MDP Formulation

In this subsection, we introduce the details of our framework in the form of MDP.

3.2.1. State

In the MDP, a state should contain necessary information that the policy network needs for decision-making at the current step. In our task for route construction, the state at decision step t , denoted as s_t , consists of two parts: 1) the TPP instance U being solved, which is *static* throughout the solving process, and 2) the *dynamic* information of the partial route that has been constructed up to step t . Specifically, the TPP instance U is represented as a bipartite graph, which will be introduced in detail in Section 4. For the dynamic information, we consider two contents that are critical to the decision task at step t :

- the nodes on the partial route $\pi^t = (v_0, v^1, v^2, \dots, v^{t-1})$,
- the remaining demand $d^t = (d_1^t, d_2^t, \dots, d_{|K|}^t)$,

where v^1, v^2, \dots, v^{t-1} denote the nodes selected at previous decision steps $1, 2, \dots, t-1$, respectively, and d_k^t denotes the remaining demand of product $k \in K$, assuming all possible quantities of product k supplied in the partial route have been purchased. In the initial state s_1 , the route starts from the depot v_0 and no products have been purchased, i.e., where $\pi^1 = (v_0)$ and $d^1 = (d_1, d_2, \dots, d_{|K|})$.

We remark that ideally, a well-trained policy network can automatically extract information about the remaining demand d^t given the instance U and the current partial route π^t , but we found that explicitly providing d^t to the policy network can effectively reduce the computational load and accelerate training. Therefore, we still include the remaining demand d^t as part of a state s_t .

3.2.2. Action

At each decision step t , an action $a_t \in A_t$ is defined as selecting the next node (i.e., a new market or the depot) to visit. If a new market is selected, the purchaser will visit it and start the next step $t+1$. Otherwise, if the depot is selected to visit again, a complete route is formed and the route construction terminates.

Note that an arbitrarily selected action may lead to infeasible solutions, either because 1) the constructed route may not be a simple cycle, or 2) the markets on the route cannot provide any feasible purchasing plan that fulfills the product demands in the second stage. Therefore, to avoid infeasibility, we introduce two masking rules over the action set A_t at each decision step t . First, in order to strictly form a simple cycle, markets already in the partial route π^t are excluded from the action set A_t . In fact, it makes no sense to revisit a market from the perspective of optimization objective: the traveling cost will increase strictly, but no savings on the purchasing cost can be made by revisiting a market. Second, to guarantee the existence of a feasible purchasing plan based on the route, we force the depot to be masked from A_t until the remaining demand $d_k^t = 0$ for all $k \in K$. In other words, the purchaser is forbidden to return to the depot unless all product demands can possibly be satisfied from the markets on the current partial route. With these two masking rules, our approach is guaranteed to produce a feasible route and purchasing plan regardless of the quality of policy.

3.2.3. Transition

Once an action a_t is determined, the state s_t will transit deterministically to a new state s_{t+1} . Specifically, if the next node v^t is a new market, it will be added to the end of the partial route π^t :

$$\pi^{t+1} = (v_0, v^1, \dots, v^{t-1}, v^t).$$

Meanwhile, for each product $k \in K$, the previously unsatisfied demand d_k^t will be replenished if product k is available at the newly visited market v^t :

$$d_k^{t+1} = \begin{cases} \max\{0, d_k^t - q_{v^t k}\}, & \text{if } v^t \in M_k, \\ d_k^t, & \text{if } v^t \notin M_k, \end{cases}$$

where $q_{v^t k}$ is the available quantity of product k supplied at market v^t . Otherwise, if the next node v^t is the depot, indicating a complete route is formed, the MDP terminates and then the reward calculation procedure for the terminal state is executed. Note that the TPP instance U , that is, the static part of the states, remains fixed throughout the state transitions in an MDP.

3.2.4. Reward

After the sequential route construction process described above, the second stage, i.e., purchase planning, is executed, which is integrated into the reward calculation procedure for the terminal state. Given the constructed route, a linear transportation problem is solved to derive the optimal purchasing plan for the visited markets. In the transportation problem, each source point corresponds to a market on the route, and each destination point corresponds to a product to be purchased. The cost to purchase a unit of product k from market i is exactly the unit transportation cost from source point i to destination point k in the transportation problem. This transportation problem can be readily solved using an off-the-shelf LP solver or a polynomial-time dynamic programming algorithm (Munkres, 1957). So far, a complete solution, including a route and the associated purchasing plan, has been obtained.

The objective of TPPs is to minimize the sum of traveling and purchasing costs while meeting all problem constraints. Since the feasibility of the route and the purchasing plan have been guaranteed by the masking rules (Section 3.2.2), we define the reward for the terminal state as the negative objective value, i.e., the sum of traveling and purchasing costs, and set zero-reward for all intermediate states. The reward is used to update the policy network through a DRL training algorithm, which will be specifically described later in Section 5.2. This way, the policy network is trained to optimize the global objective, that is, to construct a high-quality route that minimizes not only the traveling cost itself but also the subsequent purchasing cost based on it, thus to minimize the total cost.

3.2.5. Policy

Given the state s_t at each step t , the action a_t is selected according to a stochastic policy $p_\theta(a_t | s_t)$, which can be seen as an action distribution over the action set A_t . Since the transition from a state s_t to the next state s_{t+1} is deterministic given an action a_t (Section 3.2.3), the joint probability to sample a route π based on the stochastic policy $p_\theta(a_t | s_t)$ can be factorized according to the chain rule as:

$$p_\theta(\pi | U) = \prod_{t=1}^T p_\theta(a_t | s_t),$$

where the route is constructed in T steps, and the action a_t is sampled based on the policy $p_\theta(a_t | s_t)$ at each step. In our DRL-based approach, the policy is parameterized as a deep neural network θ , where the input of the policy network is the state s_t and the output is the policy, i.e., the action distribution $p_\theta(a_t | s_t)$. It can be seen that in our framework, the policy network plays a determinative role in the quality of solutions. Our training goal is to learn an effective policy network that can produce high-reward solutions with high probabilities and low-reward solutions with low probabilities.

4. Bipartite Graph Representation for TPPs

In the following sections, we will introduce the key DRL components in our framework. In this section, we first propose a novel bipartite graph representation for TPPs. The bipartite graph representation serves as an important part of the states (Section 3.2.1), which provides the policy network with global information about the TPP instance being solved.

Similar to existing DRL-based methods for routing problems (Kool et al., 2019; Fu et al., 2021), a natural and straightforward idea is to represent a TPP instance as a complete or k -NN graph,

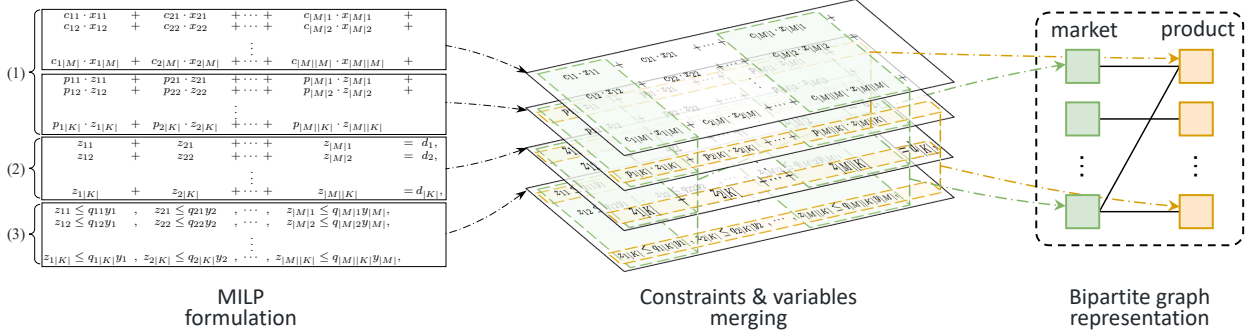


Figure 2: The bipartite graph representation for TPPs. The bipartite graph representation is built on the MILP formulation of TPPs, where the constraints or variables that are associated with the same element are merged (as the central subfigure).

where each market is represented as a node, which is connected to each other, and the product supply information at each market are represented as node features. However, despite containing necessary information for the TPP instance, such representations impose many drawbacks when used in DRL. First, the feature dimensions vary with the number of products in the TPP instance being solved. For example, considering two features for each product: the available quantity and price, a 50-product instance requires a 100-dimensional feature vector for each node to record these 50 products, while an instance with 100 products would require 200 dimensions. This will lead to a computational mismatch in the forward-propagation of neural networks. In other words, a policy network can only be applied on fixed-sized TPP instances, unable to adapt to instances with different sizes even if only one additional product is included, which significantly limits its practical usability. Second, the relations between markets and products, such as the substitutions and complementarities in product supply between different markets, are very important for constructing a low-cost route, but such information is largely ignored in the aforementioned complete or k -NN graph representations. To address these limitations, we design a novel bipartite graph representation, which is built upon the MILP formulation of TPPs (Section 2).

Bipartite graphs have been demonstrated effective in representing general MILP problems (Nair et al., 2020; Morabit et al., 2021), where the variables and constraints are represented as two sets of nodes, and an edge connects a variable node and a constraint node if the corresponding column contributes to this constraint. Readers are referred to Chen et al. (2023) for a more detailed introduction and analysis. However, directly applying this representation to the MILP formulation (1)-(9) for TPPs can introduce unnecessary redundancy: the parameters to characterize a specific TPP instance exist only in the objective function (1) and constraints (2)-(3), whereas constraints (4)-(6), which are used to form a simple cycle, have already been guaranteed by the masking rules (Section 3.2.2) and therefore need not be explicitly represented for the policy network. Moreover, the constraints and variables associated with the same element (e.g., a market or a product) can be further merged to reduce the graph size and thus improve the computational efficiency of the policy network.

Therefore, we design a bipartite graph representation for TPPs based on the objective function (1) and constraints (2)-(3), with appropriate mergence for the constraints and variables therein. Our bipartite graph representation is shown as Figure 2. We represent the constraints associated only with *products* (i.e., constraints (2)) and the variables associated only with *markets/depot*

(i.e., variables v_i and x_{ij}) as two sets of nodes, and the constraints and variables associated with *both products and markets* (i.e., constraints (3) and variables z_{ik}) as edges between the product nodes and market/depot nodes. Specifically, each variable v_i is represented as a market/depot node, and the objective coefficients c_{ij} of variables x_{ij} are represented as coordinate features of the market/depot nodes. Each constraint in (2) is represented as a product node, with the right-hand side values d_k attached as node features. An edge connects a market node i and a product node k if the associated variable z_{ik} is not always restricted to 0 in constraints (3), that is, product k is available at market i . The edge feature is a 2-dimensional vector, which consists of the corresponding objective coefficient p_{ik} of variable z_{ik} and the constraint coefficient q_{ik} in constraints (3). For simplicity in the remainder of this paper, we use the term “market nodes” to refer to “market/depot nodes” if it does not cause confusion. We remark that our bipartite graph representation can be viewed from a more intuitive perspective: the two core elements in TPPs, i.e., markets and products, are represented as two sets of nodes, and their connections, i.e., available quantities and prices of the products at the markets, are characterized using the edges between them.

We emphasize that our bipartite graph representation effectively addresses the limitations of the complete or k -NN graph representations mentioned above. First, the node and edge feature dimensions are invariant to the number of markets and products, allowing the design of a size-agnostic policy network, such that it can be flexibly adapted to TPP instances of varying sizes. Second, the bipartite graph explicitly characterizes the relations between markets and products through the edges connecting market nodes and product nodes. The message-passing along edges can effectively capture the relational information between markets and products, which is useful for the decision tasks.

5. Policy Network

In this section, we introduce the architecture of our policy network, which is used in the first stage for route construction. In addition, at the end of this section, we will describe the basic training algorithm for updating the policy network during training.

5.1. Policy Network Architecture

As aforementioned, at each decision step t , the policy network θ takes the state s_t (consisting of the TPP instance U being solved, which is represented as a bipartite graph, the partial route π^t , and the remaining demand d^t) as input, and outputs a distribution $p_\theta(a_t|s_t)$ over the actions $a_t \in A_t$ to decide the next node to visit. The architecture of our policy network is illustrated as Figure 3. The policy network is composed of 1) an input embedding module, 2) a market encoder, and 3) a decoder.

The encoding process is designed based on the structure of bipartite graph. Specifically, the input embedding module takes the bipartite graph representation of instance U as input, performing message-passing along edges and producing high-dimensional embeddings for the market and product nodes. Then, the market node embeddings are processed through the market encoder to extract further information for the TPP instance. After the encoding process, the decoder is executed iteratively to construct the route in a sequential manner. Specifically, at each decision step t , the decoder receives a decoding context, which contains the embeddings of the bipartite graph and the dynamic part of current state s_t (i.e., π^t and d^t) as input. It then outputs a distribution $p_\theta(a_t | s_t)$, i.e., the policy, from which an action a_t is selected, determining the next node to visit,

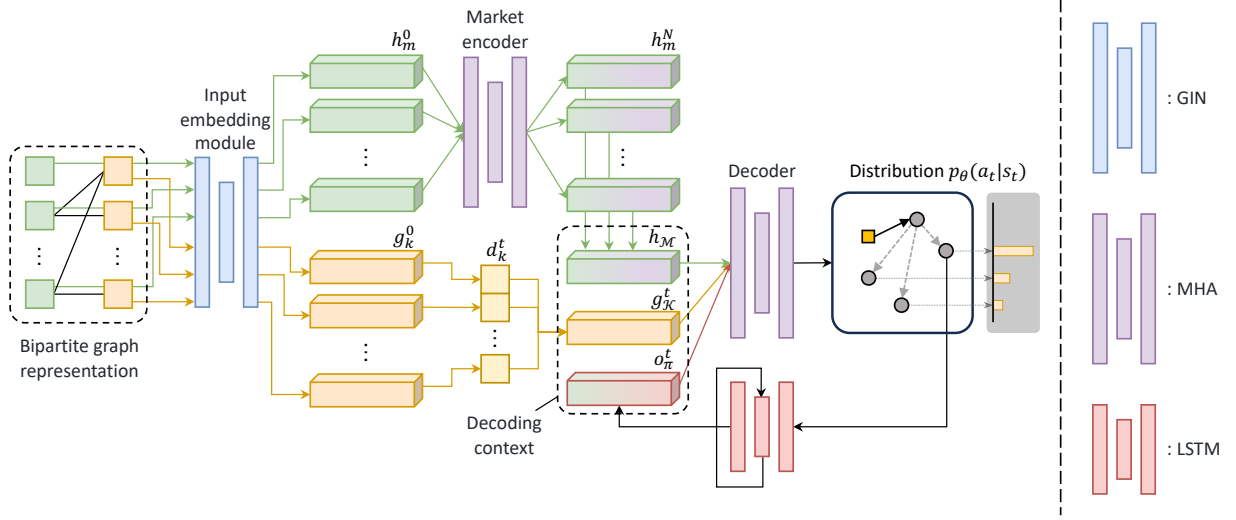


Figure 3: The architecture of our policy network. The policy network is composed of 1) an input embedding module, 2) a market encoder, and 3) a decoder. The bipartite graph is embedded through the input embedding module and the market encoder. Then, the decoder is executed iteratively: at each step t , the decoder takes as input a decoding context, and outputs an action distribution $p_\theta(a_t | s_t)$, from which an action a_t is selected, determining the next node to visit.

and the dynamic part π^t and d^t of the state are updated to start the next decoding step. Note that given a TPP instance U , the bipartite graph representation of U is fixed throughout the state transitions in a complete MDP. Therefore, we execute the input embedding module and market encoder only once in the initial state, and then execute the decoder iteratively with the decision steps of the MDP. In the following, we will present a detailed introduction to the three components of our policy network.

5.1.1. Input Embedding Module

Taking the bipartite graph representation of instance U as input, the input embedding module exploits the raw features and topology of the bipartite graph to produce a high-dimensional embedding for each market node and product node. GNN is an effective framework that naturally operates on graph-structured data and learns relational information through message-passing between the nodes on the graph (Wu et al., 2021; Cappart et al., 2023). Therefore, we leverage GNNs in the input embedding module to embed the bipartite graph and capture the relations between markets and products.

Considering the feature heterogeneity of the bipartite graph representation, we first normalize the raw node and edge features by the product demands and linearly project them into the initial embeddings with a uniform dimension. Then, based on the structure of the input bipartite graph, we design a two-phase message-passing procedure that updates the initial node embeddings by aggregating information across the market nodes and product nodes: the first phase is performed to update the embeddings of product nodes, followed by the second phase that updates the embeddings of market nodes. Specifically, let g_k^{init} , h_m^{init} and e_{km}^{init} denote the initial embeddings of product node

k , market node m , and edge (k, m) , respectively. The two-phase update is processed as follows:

$$\begin{aligned} g_k^0 &= \text{MLP}_{\mathcal{K}} \left((1 + \epsilon) \cdot g_k^{\text{init}} + \sum_{m \in \mathcal{N}(k)} \text{ReLU}(h_m^{\text{init}} + e_{mk}^{\text{init}}) \right), \\ h_m^0 &= \text{MLP}_{\mathcal{M}} \left((1 + \epsilon) \cdot h_m^{\text{init}} + \sum_{k \in \mathcal{N}(m)} \text{ReLU}(g_k^0 + e_{km}^{\text{init}}) \right), \end{aligned}$$

where $\text{MLP}_{\mathcal{K}}$ and $\text{MLP}_{\mathcal{M}}$ are multi-layer perceptrons (MLPs) for updating the product nodes and market nodes, respectively, and $\mathcal{N}(k)$ and $\mathcal{N}(m)$ denote the 1-hop neighbor node set of product node k and market node m , respectively. Both phases can be viewed as a modification of the graph isomorphism network (GIN) (Xu et al., 2019) that further takes into account the bipartite structure and incorporates edge embeddings in the update. The updated product node embeddings g_k^0 for $k = 1, 2, \dots, |K|$ and market node embeddings h_m^0 for $m = 0, 1, \dots, |M|$ are then used in the market encoder and the decoder.

We remark that our design behind the two-phase embedding procedure is intuitive: in the first phase, we make each product node collect its supply information, including in which markets it is supplied, the coordinates of these markets, as well as the supply quantities and prices; and in the second phase, we make each market node collect higher-level information about its supplied products, including not only their total demands but also the information about how these products are supplied at other markets, which is extracted based on the product node embeddings from the first phase. Consequently, the product node embedding g_k^0 aggregates its global supply information, and the market node embedding h_m^0 collects more complex information such as the substitutive and complementary relations of product supply with other markets, which is important for the market selection decisions in route construction.

5.1.2. Market Encoder

It is empirically observed from prior works for routing problems that deeper information extraction for the city nodes, i.e., market nodes in our task, can potentially improve the capability of the policy network (Kwon et al., 2020; Joshi et al., 2022). Thus, we process the market node embeddings through a market encoder for further information extraction.

Following the Transformer (Vaswani et al., 2017) architecture, we process the market node embeddings through N stacked attention layers. Each attention layer consists of two sublayers: an MHA layer that executes information aggregation for the market nodes and a node-wise MLP feed-forward layer to update the aggregated embeddings, where both sublayers add a residual connection (He et al., 2016) and batch normalization (BN) (Ioffe and Szegedy, 2015):

$$\begin{aligned} \hat{h}_m^{\ell+1} &= \text{BN}^{\ell} \left(h_m^{\ell} + \text{MHA}_m^{\ell} \left(h_0^{\ell}, \dots, h_{|M|}^{\ell} \right) \right), \\ h_m^{\ell+1} &= \text{BN}^{\ell} \left(\hat{h}_m^{\ell+1} + \text{MLP}^{\ell} \left(\hat{h}_m^{\ell+1} \right) \right), \end{aligned}$$

where $h_m^{\ell+1}$ is the embedding of market node m after layer ℓ for $\ell = 0, \dots, N - 1$. The MHA layer adopts a scaled dot-product attention mechanism, where the attention function can be viewed as a mapping from a query vector and a set of key-value pairs to an output vector. Specifically, for each attention head, a query vector q_m^{ℓ} , a key vector k_m^{ℓ} , and a value vector v_m^{ℓ} are calculated for

each market node m through a linear projection of its node embedding:

$$q_m^\ell = W_q^\ell h_m^\ell, \quad k_m^\ell = W_k^\ell h_m^\ell, \quad v_m^\ell = W_v^\ell h_m^\ell,$$

where W_q^ℓ , W_k^ℓ , and W_v^ℓ are trainable parameters. The attention output for market node m is computed as a weighted sum of the values $v_0^\ell, \dots, v_{|M|}^\ell$, where the weight assigned to each value is the scaled dot-product of the query q_m^ℓ with the corresponding keys $k_0^\ell, \dots, k_{|M|}^\ell$:

$$u_{mn}^\ell = \frac{(q_m^\ell)^\top \cdot k_n^\ell}{\sqrt{\dim_k}},$$

$$\text{Attention}^\ell(h_m^\ell) = \sum_{n=0}^{|M|} \text{softmax}(u_{mn}^\ell) \cdot v_n^\ell,$$

where \dim_k is the dimension of key vectors. Multi-head attention can be interpreted as multiple attention functions in parallel, which allows the node to collect diverse messages from other nodes through different attention heads. Then, we obtain the final MHA value of market node m through a linear projection W_o^ℓ of the concatenated attention heads:

$$\text{MHA}_m^\ell(h_0^\ell, \dots, h_{|M|}^\ell) = W_o^\ell [\text{head}_{m,1}^\ell, \dots, \text{head}_{m,H}^\ell],$$

where $\text{head}_{m,i}^\ell$ is an abbreviation for $\text{Attention}_i^\ell(h_m^\ell)$ and $[\cdot, \cdot]$ is the concatenation operator.

After the N attention layers, we compute the mean of final market node embeddings as a global embedding $h_{\mathcal{M}}$, which can be viewed as an aggregation of the final extracted information for the bipartite graph:

$$h_{\mathcal{M}} = \frac{1}{|M| + 1} \sum_{m=0}^{|M|} h_m^N.$$

The global embedding $h_{\mathcal{M}}$ is then used as part of the decoding context for the decoder.

5.1.3. Decoder

The bipartite graph of the TPP instance U is encoded through the input embedding module and market encoder. After that, the decoder is executed iteratively to construct the route, one node at a step. At each step $t = 1, 2, \dots, T$, the decoder takes as input a decoding context h_d of the state s_t , and outputs a distribution $p_\theta(a_t | s_t)$ over the actions $a_t \in A_t$. Then, an action a_t is selected based on the distribution. The corresponding market/depot is added to the end of the partial route, and the state is updated accordingly to start the next decoding step, until a complete route is constructed.

The decoding context provides the decoder with the embedded information of current state s_t , including the instance U , the partial route π^t , and the remaining demand d^t . We form the decoding context h_d as the concatenation of three parts: 1) the global embedding $h_{\mathcal{M}}$, 2) a demand context g_K^t , and 3) a route context o_π^t :

$$h_d = [h_{\mathcal{M}}, g_K^t, o_\pi^t].$$

First, as introduced above, the global embedding $h_{\mathcal{M}}$ is the aggregation of the final extracted information from the bipartite graph, which contains global information of the instance U being

solved. Second, we form the demand context $g_{\mathcal{K}}^t$ as a weighted sum of product embeddings, where the weight for each product k is its remaining demand d_k^t :

$$g_{\mathcal{K}}^t = \sum_{k=1}^{|K|} d_k^t \cdot g_k^0.$$

The demand context $g_{\mathcal{K}}^t$ contains the information of remaining demand d^t . Third, the route context o_{π}^t is the embedding for the partial route π^t , i.e., a sequence of market/depot nodes. We adopt an LSTM (Hochreiter and Schmidhuber, 1997) recurrent network, similar to the decoding RNN in Ptr-Net (Vinyals et al., 2015), to obtain the route context o_{π}^t :

$$o_{\pi}^t = \text{LSTM}(o_{\pi}^{t-1}, h_{v^t}^N),$$

where $h_{v^t}^N$ is the final embedding of the node v^t added to the partial route at the last step.

The decoder leverages the information from the decoding context h_d to make decisions. It first processes the decoding context h_d through a one-to-many attention layer, where the query is from the decoding context h_d , and the keys and values are from the final market/depot node embeddings $h_0^N, \dots, h_{|M|}^N$. Then, the action distribution $p_{\theta}(a_t | s_t)$ is computed as the single-head attention weights between the updated decoding context vector (denoted as h'_d) and the final node embeddings $h_0^N, \dots, h_{|M|}^N$ of markets/depot. We first computed attention scores between h'_d and the final market/depot node embeddings:

$$u_{dm} = \begin{cases} C \cdot \tanh\left(\frac{(q'_d)^T \cdot k_m^N}{\sqrt{\dim_k}}\right), & \text{if node } m \text{ is not masked,} \\ -\infty, & \text{otherwise,} \end{cases}$$

where the query q'_d is from the updated decoding context vector h'_d , and the keys k_m^N are from the final market/depot node embeddings h_m^N for $m = 0, \dots, |M|$. The attention scores are clipped using tanh function scaled by C , and the scores for the masked actions are set to $-\infty$. The final output distribution is computed using a softmax function:

$$p_{\theta}(a_t = m | s_t) = \frac{e^{u_{dm}}}{\sum_{n=0}^{|M|} e^{u_{dn}}}, \quad \text{for } m = 0, \dots, |M|.$$

Then, an action a_t is selected based on the distribution, and the corresponding market/depot m is added to the partial route. Specifically, we sample the action a_t from the distribution $p_{\theta}(a_t | s_t)$ during training, and select greedily the action with the maximum probability when applying the learned policy for inference.

We remark that besides its strong capability, the design of our policy network has many benefits. First, our policy network based on GNNs and MHA is agnostic to the size of instances being solved, as long as the input feature dimensions are fixed, which is achieved in our proposed bipartite graph representation. This allows the policy network to directly adapt to TPP instances with varying numbers of markets and products, without the need for parameter adjustment or retraining. Second, the embedding process for the static part U and the dynamic part π^t and d^t of a state can be separated, which improves the computational efficiency of the policy network. Specifically, the embeddings of U are pre-computed only once at the initial states using the computationally intensive input embedding module and market encoder, while the computationally light decoder

is executed repeatedly with varying decoding contexts that contain the dynamic information of states. Moreover, the forward-propagation of our policy network based on GNNs and MHA is highly parallelizable, which further improves the computational efficiency when used for solving TPPs.

5.2. Basic Training Algorithm

The policy network is updated based on the reward received after the solving process. As introduced in Section 3.2.4 and Section 3.2.5, given a TPP instance U , the policy network θ generates the final route π with probability $p_\theta(\pi | U) = \prod_{t=1}^T p_\theta(a_t | s_t)$ during training, where the associated traveling cost can be directly accessed, and the purchasing cost is obtained by solving a transportation problem. To align with the notations in DRL, we let $L(\pi | U)$ denote the loss of π , which is defined as the negative reward for the terminal state. We update the policy network θ to minimize the expectation of loss $L(\pi | U)$, using the REINFORCE algorithm (Williams, 1992) with baseline $b(U)$:

$$\nabla_\theta \mathcal{L}(\theta | U) = \mathbb{E}_{\pi \sim p_\theta(\pi | U)} [(L(\pi | U) - b(U)) \nabla_\theta \log p_\theta(\pi | U)],$$

where the baseline $b(U)$ can be seen as an estimation for the difficulty of instance U to measure the relative advantage of route π generated by the policy network. A well-defined baseline can significantly reduce the variance of gradients and accelerate training. We define the baseline $b(U)$ as the loss of the route obtained from a deterministic greedy rollout, i.e., where the action with the highest probability is always selected at each decision step, based on a baseline network θ^{BL} (Kool et al., 2019). Similar to the target Q-network in DQN (Mnih et al., 2015), the baseline network θ^{BL}

Algorithm 1: REINFORCE algorithm with greedy rollout baseline

Input: Initial policy network parameter θ ,
TPP instance distribution \mathcal{P} ,
number of epochs E , batch size B ,
steps per epoch T , learning rate ϵ ,
significance α .

Output: The learned policy network parameter θ .
Initialize baseline network parameter $\theta^{\text{BL}} \leftarrow \theta$;

for $e = 1, \dots, E$ **do**

for $t = 1, \dots, T$ **do**

Generate B instances randomly from \mathcal{P} ;

Sample route $\pi_i \sim p_\theta(\pi_i | U_i)$, $i \in \{1, \dots, B\}$;

Greedy rollout $b(U_i)$ from $p_{\theta^{\text{BL}}}$, $i \in \{1, \dots, B\}$; // compute baseline

$\nabla \mathcal{L} \leftarrow \sum_{i=1}^B (L(\pi_i | U_i) - b(U_i)) \nabla_\theta \log p_\theta(\pi_i | U_i)$; // get gradient

$\theta \leftarrow \text{Adam}(\theta, \nabla \mathcal{L})$; // update policy network

end

if $\text{OneSidedPairedTTest}(p_\theta, p_{\theta^{\text{BL}}}) < \alpha$ **then**

$\theta^{\text{BL}} \leftarrow \theta$; // update baseline network

end

end

is a copy of policy network θ , but is fixed during each epoch to stabilize the baseline value. The baseline network θ^{BL} is periodically replaced by the latest policy network θ if the improvement of the policy is significant enough according to a paired t-test. Based on the gradient $\nabla_{\theta} \mathcal{L}(\theta | U)$, the parameters of policy network are updated using the Adam optimizer (Kingma and Ba, 2015). The basic training algorithm introduced above is outlined as Algorithm 1.

6. Meta-learning Strategy

Despite our proposed framework and the key DRL components introduced above, how to effectively learn a high-quality policy remains another challenge, especially on large-sized TPP instances. First, due to the huge state-action space for solving TPPs, the training suffers heavily from low sample efficiency. The policy network often makes random and suboptimal actions in the early training stage, requiring substantial trial-and-error before a good policy can be found. More seriously, when trained on large-sized TPP instances, a randomly initialized policy network may completely fail to find an effective or even reasonable solution and result in training collapse (see Figure 4(b)). Second, while a well-trained policy can produce high-quality solutions for TPP instances from the same distribution as training, it tends to exhibit poor generalization performance on instances from different distributions. Generalization across different instance distributions is a highly desirable property for learning-based methods for solving CO problems.

In our approach, we address these limitations by pre-training an initialized policy network on a collection of varying instance distributions, such that it can take advantage of priorly learned cross-distribution knowledge and thus efficiently adapt to a new instance distribution using only a small amount of instances from that distribution for fine-tuning. Specifically, we propose a meta-learning strategy to learn such an initialized policy network. We consider a collection of instance distributions $\mathcal{D}_{\text{TPP}} = \{\mathcal{P}_i\}_{i=1}^D$, where each \mathcal{P}_i defines a specific instance distribution (e.g., instances sharing the same number of markets and products). In our meta-training strategy, the training process comprises an outer-loop and several inner-loop optimizations at each iteration, corresponding to pre-training an initialized policy network and fine-tuning on a specific instance distribution, respectively. The outer-loop maintains a meta policy network θ , which serves as the initialization θ_{in}^0 for the inner-loop policy network. The inner-loop fine-tunes the policy network θ_{in}^0 by performing N updates on a specific instance distribution \mathcal{P}_{in} , which is drawn from \mathcal{D}_{TPP} according to a sampling probability $p(\mathcal{D}_{\text{TPP}}) = \{p(\mathcal{P}_i)\}_{i=1}^D$ (discrete uniform distribution in our implementation). The meta-objective is to learn a meta policy network θ , which is a good initialization that can achieve low loss when adapting to a new instance distribution through N fine-tuning updates:

$$\theta^* = \arg \min_{\theta} \mathbb{E}_{\mathcal{P}_{\text{in}} \sim p(\mathcal{D}_{\text{TPP}})} \mathbb{E}_{U \sim \mathcal{P}_{\text{in}}} \mathcal{L}(\theta_{\text{in}}^N | U),$$

where θ_{in}^N is the fine-tuned inner-loop policy network after N updates from the initialization θ_{in}^0 .

In the inner-loop, we use the basic training algorithm (Section 5.2) to update the policy network N times to obtain θ_{in}^N from θ_{in}^0 . To optimize the meta-objective, we validate the fine-tuned inner-loop policy network on a validation batch $\{U'_i\}_{i=1}^B$, which is sampled from the same instance distribution \mathcal{P}_{in} as the inner-loop training. The meta-gradient to update the meta policy network θ is according to the gradient chain rule as follows:

$$\nabla_{\theta} \mathcal{L}(\theta_{\text{in}}^N) = \frac{1}{B} \sum_{i=1}^B \nabla_{\theta_{\text{in}}^N} \mathcal{L}(\theta_{\text{in}}^N | U'_i) \cdot \frac{\partial \theta_{\text{in}}^N}{\partial \theta_{\text{in}}^0}.$$

Unfortunately, the meta-gradient involves a second-order derivative in $\frac{\partial \theta_{\text{in}}^N}{\partial \theta_{\text{in}}^0}$, which is significantly expensive in computation. Therefore, we instead employ a computationally efficient first-order approximation for the meta-gradient. The update for the meta policy network is approximated as moving towards the parameters of the final inner-loop policy network (Nichol et al., 2018):

$$\theta \leftarrow \theta + \beta (\theta_{\text{in}}^N - \theta),$$

where β is the outer-loop step size. The procedure of our meta-learning strategy is outlined as Algorithm 2.

Through meta-training, the meta policy network can serve as an effective initialization that achieves good performance on a new instance distribution through a few fine-tuning steps, even on large-sized instances that tend to experience training collapse if the policy network is trained from scratch. Moreover, the meta policy network can learn cross-distribution knowledge through meta-learning, thus generalizing well across varied instance sizes and distributions, even showing good zero-shot generalization performance on instances from a different distribution that is never seen during training.

Algorithm 2: Meta-training for the policy network

Input: Initial meta policy network parameter θ ,
 TPP instance distributions set \mathcal{D}_{TPP} ,
 number of epochs E , batch size B ,
 outer steps per epoch T , outer step size β ,
 inner steps per outer-loop N , learning rate ϵ ,
 significance α .

Output: The trained meta policy network parameter θ .

Initialize baseline network parameter $\theta^{\text{BL}} \leftarrow \theta$;

for $e = 1, \dots, E$ **do**

for $t = 1, \dots, T$ **do**

 Select a distribution $\mathcal{P}_{\text{in}} \sim p(\mathcal{D}_{\text{TPP}})$; // start inner-loop

 Initialize inner model $\theta_{\text{in}} \leftarrow \theta$;

for $n = 1, \dots, N$ **do**

 Generate B instances randomly from \mathcal{P}_{in} ;

 Sample route $\pi_i \sim p_{\theta_{\text{in}}}(\pi_i | U_i)$, $i \in \{1, \dots, B\}$;

 Greedy rollout $b(U_i)$ from $p_{\theta^{\text{BL}}}$, $i \in \{1, \dots, B\}$; // compute baseline

$\nabla \mathcal{L} \leftarrow \sum_{i=1}^B (L(\pi_i | U_i) - b(U_i)) \nabla_{\theta_{\text{in}}} \log p_{\theta_{\text{in}}}(\pi_i | U_i)$; // get gradient

$\theta_{\text{in}} \leftarrow \text{Adam}(\theta_{\text{in}}, \nabla \mathcal{L})$; // inner-loop update

end

$\theta \leftarrow \theta + \beta (\theta_{\text{in}} - \theta)$; // outer-loop update

end

if $\text{OneSidedPairedTTest}(p_{\theta}, p_{\theta^{\text{BL}}}) < \alpha$ **then**

$\theta^{\text{BL}} \leftarrow \theta$;

end

end

7. Experiments

We conduct extensive experiments on various synthetic TPP instances and the TPPLIB benchmark to evaluate our DRL-based approach, comparing it with several well-established TPP heuristics. Additionally, we further confirm the zero-shot generalization ability of our policy network on larger-sized TPP instances that are unseen during training.

7.1. Experimental Settings

7.1.1. Instances

We first randomly generate synthetic TPP instances of sizes $(|M|, |K|) = (50, 50), (50, 100), (100, 50),$ and $(100, 100)$ for training and evaluation, where $|M|$ is the number of markets and $|K|$ is the number of products. The generation of U-TPP and R-TPP instances follows the standard procedure introduced in (Laporte et al., 2003), corresponding to Class 3 and Class 4 in the TPPLIB benchmark (Riera-Ledesma, 2012). For the U-TPP instance, $(|M| + 1)$ integer coordinates (including the depot) are randomly generated within the $[0, 1000] \times [0, 1000]$ square according to a uniform distribution, and the traveling costs are defined as the truncated Euclidean distances. Each product $k \in K$ is supplied at $|M_k|$ randomly selected markets, where $|M_k|$ is uniformly generated in $[1, |M|]$. The price p_{ik} for each product $k \in K$ and each market $i \in M_k$ is randomly sampled in $[1, 10]$. The R-TPP instances are generated in the similar manner as U-TPP, with an additional limit q_{ik} on the available supply quantities, which is randomly sampled in $[1, 15]$ for each product $k \in K$ and each market $i \in M_k$. A parameter λ is used to control the number of markets in a feasible solution through the product demand $d_k := \left\lceil \lambda \max_{i \in M_k} q_{ik} + (1 - \lambda) \sum_{i \in M_k} q_{ik} \right\rceil$ for $k \in K$, where $0 < \lambda < 1$. We employ $\lambda = \{0.99, 0.95, 0.9\}$ in our experiments, corresponding to the most difficult instances in the TPPLIB (Manerba et al., 2017).

We define the U-TPP instances sharing the same $(|M|, |K|)$, or the R-TPP instances sharing the same $(|M|, |K|, \lambda)$ as an instance distribution. For each instance distribution, training instances are generated on-the-fly, and a set of 1000 instances are generated for evaluation. Moreover, we further generate larger-sized instances for evaluating the zero-shot generalization ability of the policy network, which is trained on smaller instances. In addition to the synthetic instances, the well-known TPPLIB benchmark is also used for evaluation, which includes 5 instances for each instance distribution, called a category.

7.1.2. Baseline Methods

We select several well-established TPP heuristics reported in (Manerba et al., 2017), including GSH, CAH, and TRH. A widely used and effective practice is to incorporate constructive heuristics (e.g., GSH and CAH) with TRH to remove redundant markets as soon as a solution is produced. Additionally, the solution can potentially be further improved by using a TSP solver to re-sequence the order of visited markets. In our experiment, we employ GSH and CAH, both followed by TRH and the TSP re-sequence, as the baselines, denoted as “GSH+TRH” and “CAH+TRH”, respectively.

Note that we do not include exact methods in the evaluation on synthetic instances since it can take several days to weeks to solve an evaluation instance set using exact methods (even for U-TPP). For a comparison of the optimality gap, we report the best-known solutions in the literature (Riera-Ledesma, 2012) on the TPPLIB benchmark instances to assess the optimality gaps of the baseline heuristics and our DRL-based approach.

Hyper-parameter	Value
Embedding dimension	128
Num of market encoder layers	3
Key vector dimension	16
Num of attention heads	8
Clipping scale for tanh	10.0
Num of epochs	100
Batch size	512
Steps per epoch	2500
Learning rate	1e-4
T-test significance	0.05
Outer steps per epoch	2500
Inner steps per outer-loop	2
Outer step size	0.8

Table 1: Training configuration.

7.1.3. Training and Inference of the Policy Network

The detailed training configuration for the policy network is presented in Table 1. Both training and inference are performed on a machine equipped with an AMD EPYC 7742 CPU at 2.3 GHz and a single GeForce RTX-4090 GPU.

In the evaluation of our DRL-based approach, we execute the inference of the learned policy network with greedy decoding (similar to the greedy rollout baseline) and instance augmentation (Kwon et al., 2020). The produced route and purchasing plan can be directly used as an end-to-end solution to the TPP instance, denoted as “RL-E2E”. Similar to the baseline heuristics, this end-to-end solution can be further improved through a post-optimization procedure (TRH and TSP re-sequence), denoted as “RL+TRH”. For a fair comparison, the baseline heuristics and our approach are implemented on the same machine and environment.

7.2. Training Performance

First, we present the training performance of the policy network on different instance distributions, highlighting the necessity and effectiveness of our meta-learning strategy.

The policy network is trained from scratch for U-TPP and R-TPP instances of sizes $(|M|, |K|) = (50, 50)$ and $(50, 100)$. For brevity, we illustrate the training curve on U-TPP instances of size $(|M|, |K|) = (50, 50)$ in Figure 4(a), which is plotted based on the average loss on the evaluation instance set. The stable convergence demonstrates that our policy network is capable of learning an effective policy for small-sized TPPs when trained from scratch using the basic training algorithm.

However, the policy network suffers serious training collapse when trained from scratch on large-sized U-TPP and R-TPP instances of sizes $(|M|, |K|) = (100, 50)$ and $(100, 100)$. As shown in Figure 4(b), the policy network trained from scratch on U-TPP instances of size $(|M|, |K|) = (100, 50)$ is stuck in a high-loss region, and the loss completely fails to decrease throughout training. This is mainly because the state-action space is so large that the policy network cannot find an effective or even reasonable solution if the training starts from a random initialization. Therefore, we instead apply our meta-learning strategy to train the policy network for U-TPP and R-TPP instances with $(|M|, |K|) = (100, 50)$ and $(100, 100)$. As shown in Figure 4(b), the utilization of meta-learning strategy significantly promotes the training for an effective policy.

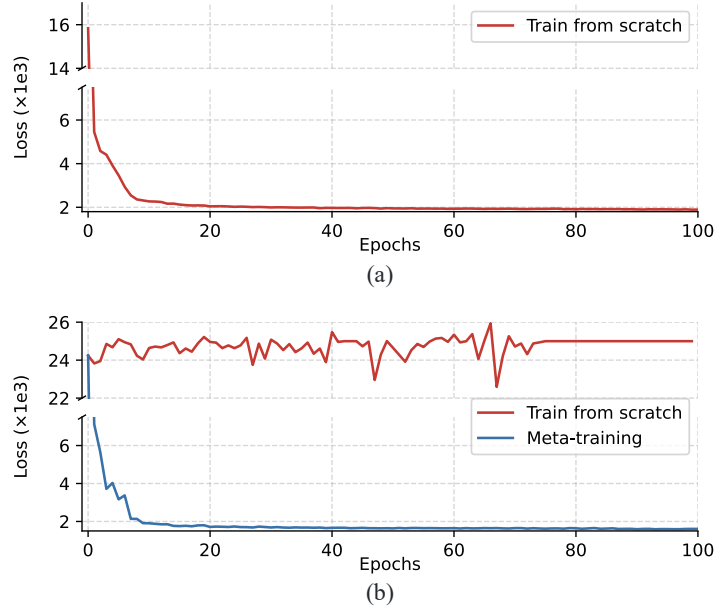


Figure 4: The training curve on (a) U-TPP instances of size $(|M|, |K|) = (50, 50)$, and (b) U-TPP instances of size $(|M|, |K|) = (100, 50)$

7.3. Results on Synthetic Instances

Following the training procedures described above, we train the policy network from scratch for U-TPP and R-TPP instances of sizes $(|M|, |K|) = (50, 50)$ and $(50, 100)$, and apply the meta-learning strategy for training U-TPP and R-TPP instances of sizes $(|M|, |K|) = (100, 50)$ and $(100, 100)$. Then, the learned policy network is evaluated on the set of 1000 synthetic evaluation instances for each instance distribution. We report the metrics of 1) the average objective value and 2) the runtime (in seconds) for each evaluation instance set. The results are reported in Table 2 for U-TPP and Table 3 for R-TPP.

In terms of the objective value, the performance of baseline heuristics varies across different instance distributions. In comparison, our DRL-based approach consistently outperforms both GSH+TRH and CAH+TRH on all synthetic U-TPP and R-TPP instance sets of different sizes and distributions. Notably, the end-to-end solutions (RL-E2E) can already achieve better objective value than the hand-crafted baseline heuristics, and the post-optimization procedure (RL+TRH) further improves the solution, with only a slight increase in solution time. The results demonstrate that our DRL-based approach is able to learn effective policies for solving TPPs of different sizes and distributions.

In terms of the runtime, all baseline heuristics and our DRL-based approach can produce a solution within an average of 0.1 seconds for U-TPP instances of all four sizes. In general, GSH+TRH takes the least time, but the advantage is approximately negligible in practice. However, for more challenging R-TPP instances, the solution time of baseline heuristics increases significantly with the instance size, as shown in Figure 5(b)-(d). GSH+TRH and CAH+TRH take an average of 1.666 seconds and 2.637 seconds, respectively, to produce a solution for R-TPP instances with $|M| = 100, |K| = 100, \lambda = 0.9$. This is mainly because they need to frequently compute the objective values and savings each time a new market is inserted into the route. In contrast, the

actions in our DRL-based approach are entirely based on the forward-propagation of the policy network. Therefore, the solution time is approximately linear with the number of visited markets in the constructed route. On synthetic R-TPP instances, the average solution time of RL-E2E is consistently less than 0.1 seconds, and the average solution time of RL+TRH is consistently less than 0.2 seconds.

Instance		GSH + TRH		CAH + TRH		RL - E2E		RL + TRH	
$ M $	$ K $	Obj.	Time	Obj.	Time	Obj.	Time	Obj.	Time
50	50	2221	0.006	1910	0.017	1897	0.017	1857	0.024
50	100	2750	0.008	2552	0.033	2542	0.025	2446	0.033
100	50	2050	0.011	1571	0.033	1563	0.020	1524	0.027
100	100	2542	0.016	2185	0.072	2111	0.027	2044	0.036

Table 2: Results on synthetic U-TPP instances.

Instance			GSH + TRH		CAH + TRH		RL - E2E		RL + TRH	
$ M $	$ K $	λ	Obj.	Time	Obj.	Time	Obj.	Time	Obj.	Time
50	50	0.99	2152	0.016	2257	0.073	2032	0.020	1954	0.030
50	100	0.99	2671	0.032	2863	0.161	2567	0.026	2466	0.042
100	50	0.99	2062	0.058	2174	0.243	1753	0.029	1711	0.043
100	100	0.99	2578	0.142	2853	0.704	2302	0.033	2235	0.053
50	50	0.95	2845	0.044	2914	0.124	2645	0.025	2594	0.036
50	100	0.95	3569	0.095	3709	0.243	3457	0.034	3368	0.059
100	50	0.95	3384	0.300	3440	0.598	3027	0.040	2980	0.073
100	100	0.95	4281	0.696	4405	1.499	3993	0.053	3920	0.111
50	50	0.9	3910	0.099	3965	0.201	3704	0.033	3644	0.052
50	100	0.9	5080	0.195	5137	0.350	4927	0.043	4855	0.080
100	50	0.9	5293	0.789	5310	1.218	4956	0.060	4900	0.124
100	100	0.9	6963	1.666	7014	2.637	6672	0.073	6660	0.186

Table 3: Results on synthetic R-TPP instances.

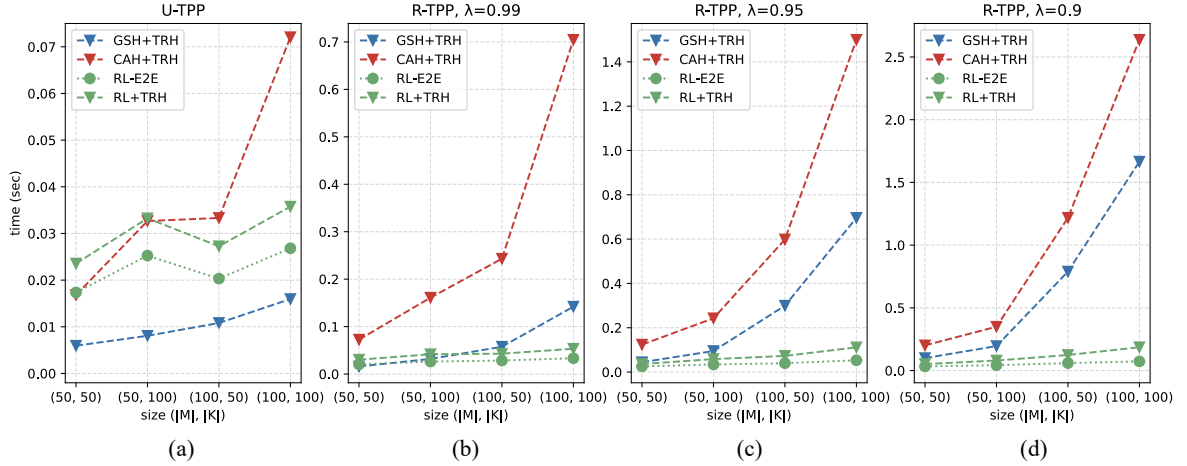


Figure 5: The runtime of the baseline methods and our DRL-based approach on the synthetic (a) U-TPP, (b) R-TPP with $\lambda = 0.99$, (c) R-TPP with $\lambda = 0.95$, and (d) R-TPP with $\lambda = 0.9$ instances.

7.4. Results on TPPLIB Benchmark Instances

Then, we evaluate our approach on the TPPLIB benchmark, by directly running the policy network (trained on synthetic instances) on the benchmark instances. The TPPLIB benchmark contains 5 instances for each instance distribution as a category. The results are summarized in Table 4. The first block of the table (prefixed with “EEuclidean”) reports the results on U-TPP instances, and the following three blocks (prefixed with “CapEuclidean”) report the results on R-

Instance	Opt.		GSH + TRH			CAH + TRH			RL - E2E			RL + TRH		
	Obj.	Time	Obj.	Gap	Time	Obj.	Gap	Time	Obj.	Gap	Time	Obj.	Gap	Time
EEuclidean.50.50	1482	4	1779	17.20%	0.007	1643	9.97%	0.015	1524	2.63%	0.014	1497	1.06%	0.019
EEuclidean.50.100	2417	6	2652	9.74%	0.008	2726	13.82%	0.032	2588	7.01%	0.025	2446	1.03%	0.037
EEuclidean.100.50	1655	72	1979	24.89%	0.009	1796	9.45%	0.031	1701	2.96%	0.019	1688	2.30%	0.027
EEuclidean.100.100	2085	183	2388	15.47%	0.013	2251	8.65%	0.075	2220	7.09%	0.025	2146	2.99%	0.064
CapEuclidean.50.50.99	1862	6	2189	20.86%	0.017	2243	23.72%	0.089	2047	9.09%	0.020	1929	3.51%	0.027
CapEuclidean.50.100.99	2313	7	2578	12.30%	0.031	2710	18.23%	0.160	2483	7.18%	0.025	2394	3.33%	0.033
CapEuclidean.100.50.99	1504	58	1951	29.97%	0.061	1988	35.73%	0.179	1561	3.91%	0.025	1531	1.84%	0.034
CapEuclidean.100.100.99	1865	134	2283	21.76%	0.118	2406	27.95%	0.686	1955	4.86%	0.028	1914	2.79%	0.039
CapEuclidean.50.50.95	2444	10	2904	21.16%	0.036	2751	15.61%	0.104	2643	7.40%	0.028	2581	5.09%	0.040
CapEuclidean.50.100.95	3187	23	3441	7.97%	0.072	3672	15.75%	0.234	3421	7.35%	0.036	3299	3.56%	0.054
CapEuclidean.100.50.95	2860	466	3144	9.85%	0.199	3221	12.73%	0.629	3026	5.93%	0.039	2962	3.66%	0.063
CapEuclidean.100.100.95	3555	1178	3991	12.31%	0.521	4096	15.24%	1.249	3769	5.94%	0.049	3664	3.00%	0.094
CapEuclidean.50.50.9	3571	28	3927	10.05%	0.061	3873	8.49%	0.145	3744	4.73%	0.036	3673	2.81%	0.053
CapEuclidean.50.100.9	4668	30	4961	6.33%	0.128	5046	8.07%	0.289	4876	4.47%	0.043	4834	3.57%	0.067
CapEuclidean.100.50.9	4674	243	4981	6.64%	0.439	5106	9.26%	0.999	4891	4.66%	0.053	4825	3.25%	0.097
CapEuclidean.100.100.9	6442	537	6961	8.11%	1.668	6850	6.43%	2.307	6637	3.01%	0.070	6534	1.42%	0.156

Table 4: Results on TPPLIB benchmark instances.

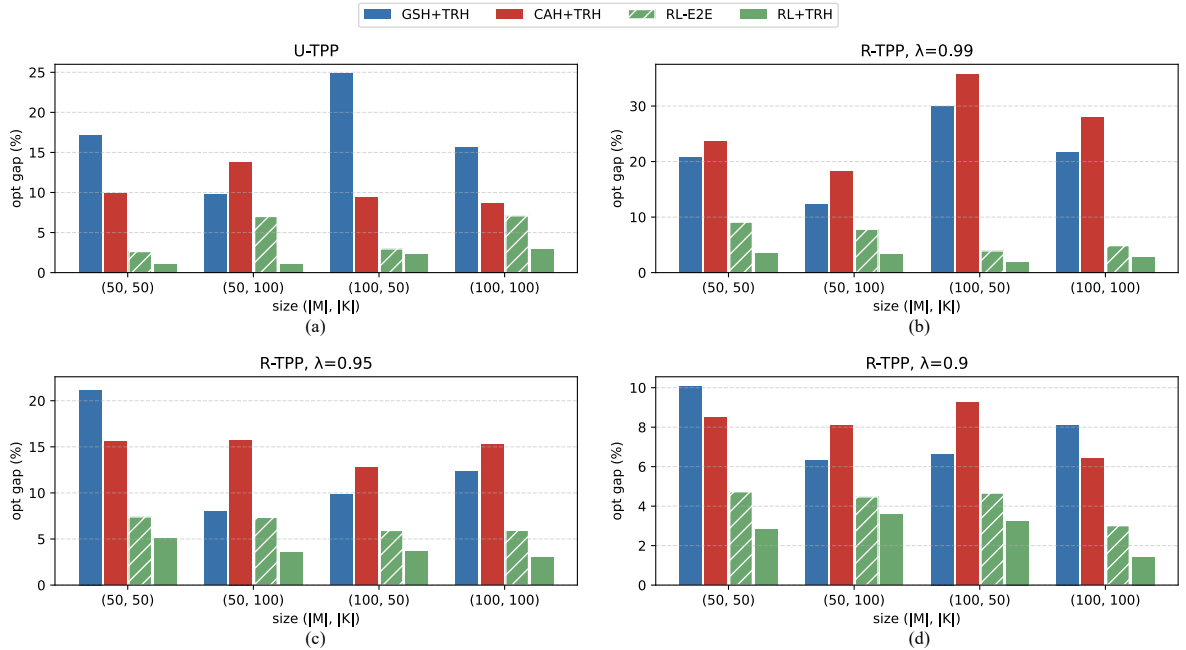


Figure 6: The optimality gaps of the baseline methods and our DRL-based approach on (a) U-TPP, (b) R-TPP with $\lambda = 0.99$, (c) R-TPP with $\lambda = 0.95$, and (d) R-TPP with $\lambda = 0.9$ in the TPPLIB benchmark.

TPP instances with $\lambda = 0.99, 0.95, 0.9$, respectively. Each row presents the average result on a category of 5 benchmark instances. For example, “CapEuclidean.50.100.95” denotes the R-TPP instances with $|M| = 50, |K| = 100, \lambda = 0.95$. We report 1) the average objective value, 2) the optimality gap, and 3) the runtime (in seconds) for each category of the TPPLIB benchmark.

The results demonstrate that the policy network, trained on synthetic instances, can be effectively applied to TPPLIB benchmark instances from the same instance distribution. Our DRL-based approach outperforms the baseline heuristics by a large margin in terms of the optimality gap, especially for large-sized R-TPP instances. In detail, the average optimality gaps of solutions produced using our RL+TRH method are consistently within 6% on each category of the TPPLIB benchmark in the experiment, yielding a reduction ranging from 40% to 90% compared to the baseline heuristics. The comparison of optimality gaps is illustrated in Figure 6. Besides, similar to the results on synthetic instances, our DRL-based approach also shows a significant advantage over the baseline heuristics in terms of the runtime.

7.5. Generalization Performance on Large-Sized Instances

Finally, we examine the zero-shot generalization performance of our approach. We use the meta-learning strategy to train the policy network on TPP instances of sizes $(|M|, |K|) = (50, 50), (50, 100), (100, 50)$, and $(100, 100)$, and then directly apply the meta policy network to solve larger-sized problem instances that are never seen in the training stage (without any fine-tuning). The results are summarized in Table 5. The first block of Table 5 presents the results on U-TPP instances of sizes $(|M|, |K|) = (150, 150), (200, 200)$, and $(300, 300)$, and the second block presents the results on R-TPP instances with $|M| = 150, |K| = 150$ and $\lambda = 0.99, 0.95, 0.9$.

It is demonstrated that our DRL-based approach still shows an advantage over the baseline heuristics when generalizing to U-TPP instances of sizes $(|M|, |K|) = (150, 150)$ and $(200, 200)$, while the largest instances for training are only of size $(|M|, |K|) = (100, 100)$. However, we observe a drop in the zero-shot generalization performance on U-TPP instances of size over $(|M|, |K|) = (300, 300)$ and R-TPP instances of size over $(|M|, |K|) = (150, 150)$. In future work, we shall further explore the generalization and more efficient transfer learning approaches for larger-sized TPP instances.

Instance			GSH + TRH		CAH + TRH		RL - E2E		RL + TRH	
$ M $	$ K $	λ	Obj.	Time	Obj.	Time	Obj.	Time	Obj.	Time
150	150	/	2672	0.027	2460	0.190	2514	0.028	2380	0.075
200	200	/	2885	0.034	2454	0.259	2485	0.040	2262	0.142
300	300	/	3445	0.041	3074	0.373	3206	0.045	3088	0.198
150	150	0.99	2918	0.265	3056	1.202	2576	0.039	2519	0.063
150	150	0.95	5642	1.318	5884	1.862	6133	0.074	6014	0.150
150	150	0.9	10008	3.027	10199	4.908	10707	0.095	10155	0.205

Table 5: Results on larger-sized instances.

8. Conclusion

In this paper, we have presented a novel DRL-based approach for solving TPPs, which exploits the idea of “*solve separately, learn globally*”. Namely, we break the solution task into two separate stages at the operating level: route construction and purchase planning, while learning

a policy network towards optimizing the global solution objective. Built on this framework, we proposed a bipartite graph representation for TPPs and designed a policy network that effectively extracts information from the bipartite graph for route construction. Moreover, we introduced a meta-learning strategy, which significantly enhances the training stability and efficiency on large-sized instances and improves the generalization ability. Experimental results demonstrate that our DRL-based approach can significantly outperform well-established TPP heuristics in both solution quality and runtime, while also showing good generalization performance. Future works shall further explore better and more efficient generalization to larger-sized TPP instances and a more generic framework to address other TPP variants, such as multi-vehicle TPP, dynamic TPP, etc.

Acknowledgments

This work was supported by the National Natural Science Foundation of China [Grants 61936009 and 42327901], and was supported by the Research and Development Project of *Lenovo Group Ltd.* and the Research and Development Project of *CRSC Research & Design Institute Group Co., Ltd.*

References

- Angelelli, E., Mansini, R., Vindigni, M., 2016. The stochastic and dynamic traveling purchaser problem. *Transportation Science* 50, 642–658.
- Bello, I., Pham, H., Le, Q.V., Norouzi, M., Bengio, S., 2017. Neural combinatorial optimization with reinforcement learning, in: *International Conference on Learning Representations*.
- Bengio, Y., Lodi, A., Prouvost, A., 2021. Machine learning for combinatorial optimization: A methodological tour d’horizon. *European Journal of Operational Research* 290, 405–421.
- Burkard, R.M., 1966. A heuristic method for a job-scheduling problem. *Journal of the Operational Research Society* 17, 291–304.
- Cappart, Q., Chételat, D., Khalil, E.B., Lodi, A., Morris, C., Velickovic, P., 2023. Combinatorial optimization and reasoning with graph neural networks. *Journal of Machine Learning Research* 24, 1–61.
- Chen, Z., Liu, J., Wang, X., Yin, W., 2023. On representing mixed-integer linear programs by graph neural networks, in: *International Conference on Learning Representations*.
- Fajemisin, A.O., Maragno, D., den Hertog, D., 2024. Optimization with constraint learning: A framework and survey. *European Journal of Operational Research* 314, 1–14.
- Finn, C., Abbeel, P., Levine, S., 2017. Model-agnostic meta-learning for fast adaptation of deep networks, in: *International Conference on Machine Learning*.
- Fu, Z., Qiu, K., Zha, H., 2021. Generalize a small pre-trained model to arbitrarily large tsp instances, in: *AAAI Conference on Artificial Intelligence*.
- Gao, H., Zhou, X., Xu, X., Lan, Y., Xiao, Y., 2024. Amarl: An attention-based multiagent reinforcement learning approach to the min-max multiple traveling salesmen problem. *IEEE Transactions on Neural Networks and Learning Systems* 35, 9758–9772.
- Goldbarg, M.C., Bagi, L.B., Goldbarg, E.F.G., 2009. Transgenetic algorithm for the traveling purchaser problem. *European Journal of Operational Research* 199, 36–45.
- Golden, B., Levy, L., Dahl, R., 1981. Two generalizations of the traveling salesman problem. *Omega* 9, 439–441.
- He, K., Zhang, X., Ren, S., Sun, J., 2016. Deep residual learning for image recognition, in: *IEEE Conference on Computer Vision and Pattern Recognition*.
- Hochreiter, S., Schmidhuber, J., 1997. Long short-term memory. *Neural Computation* 9, 1735–1780.
- Ioffe, S., Szegedy, C., 2015. Batch normalization: Accelerating deep network training by reducing internal covariate shift, in: *International Conference on Machine Learning*.
- Joshi, C.K., Cappart, Q., Rousseau, L., Laurent, T., 2022. Learning the travelling salesperson problem requires rethinking generalization. *Constraints* 27, 70–98.
- Kalatzantonakis, P., Sifaleras, A., Samaras, N., 2023. A reinforcement learning-variable neighborhood search method for the capacitated vehicle routing problem. *Expert Systems with Applications* 213, 118812.
- Kim, M., Park, J., Park, J., 2022. Sym-nco: Leveraging symmetry for neural combinatorial optimization, in: *Advances in Neural Information Processing Systems*.

- Kingma, D.P., Ba, J., 2015. Adam: A method for stochastic optimization, in: International Conference on Learning Representations.
- Kool, W., van Hoof, H., Welling, M., 2019. Attention, learn to solve routing problems!, in: International Conference on Learning Representations.
- Kwon, Y., Choo, J., Kim, B., Yoon, I., Gwon, Y., Min, S., 2020. POMO: policy optimization with multiple optima for reinforcement learning, in: Advances in Neural Information Processing Systems.
- Laporte, G., Riera-Ledesma, J., González, J.J.S., 2003. A branch-and-cut algorithm for the undirected traveling purchaser problem. *Operations Research* 51, 940–951.
- Lopes Silva, M.A., de Souza, S.R., Freitas Souza, M.J., Bazzan, A.L.C., 2019. A reinforcement learning-based multi-agent framework applied for solving routing and scheduling problems. *Expert Systems with Applications* 131, 148–171.
- Manerba, D., Mansini, R., Riera-Ledesma, J., 2017. The traveling purchaser problem and its variants. *European Journal of Operational Research* 259, 1–18.
- Mnih, V., Kavukcuoglu, K., Silver, D., Rusu, A.A., Veness, J., Bellemare, M.G., Graves, A., Riedmiller, M.A., Fidjeland, A., Ostrovski, G., Petersen, S., Beattie, C., Sadik, A., Antonoglou, I., King, H., Kumaran, D., Wierstra, D., Legg, S., Hassabis, D., 2015. Human-level control through deep reinforcement learning. *Nature* 518, 529–533.
- Morabit, M., Desaulniers, G., Lodi, A., 2021. Machine-learning-based column selection for column generation. *Transportation Science* 55, 815–831.
- Munkres, J., 1957. Algorithms for the assignment and transportation problems. *Journal of the Society for Industrial and Applied Mathematics* 5, 32–38.
- Nair, V., Bartunov, S., Gimeno, F., Von Glehn, I., Lichocki, P., Lobov, I., O’Donoghue, B., Sonnerat, N., Tjandraatmadja, C., Wang, P., et al., 2020. Solving mixed integer programs using neural networks. *arXiv preprint arXiv:2012.13349*.
- Nazari, M., Oroojlooy, A., Snyder, L.V., Takác, M., 2018. Reinforcement learning for solving the vehicle routing problem, in: Advances in Neural Information Processing Systems.
- Nichol, A., Achiam, J., Schulman, J., 2018. On first-order meta-learning algorithms. *arXiv preprint arXiv:1803.02999*.
- Ong, H.L., 1982. Approximate algorithms for the travelling purchaser problem. *Operations Research Letters* 1, 201–205.
- Palomo-Martínez, P.J., Salazar-Aguilar, M.A., 2019. The bi-objective traveling purchaser problem with deliveries. *European Journal of Operational Research* 273, 608–622.
- Pearn, W.L., Chien, R.C., 1998. Improved solutions for the traveling purchaser problem. *Computers & Operations Research* 25, 879–885.
- Que, Q., Yang, F., Zhang, D., 2023. Solving 3d packing problem using transformer network and reinforcement learning. *Expert Systems with Applications* 214, 119153.
- Ramesh, T., 1981. Travelling purchaser problem. *Opsearch* 18, 78–91.
- Riera-Ledesma, J., 2012. TPPLIB. URL <https://jriera.webs.ull.es/TPP.htm/>.
- Riera-Ledesma, J., González, J.J.S., 2006. Solving the asymmetric traveling purchaser problem. *Annals of Operations Research* 144, 83–97.
- Rodríguez-Esparza, E., Masegosa, A.D., Oliva, D., Onieva, E., 2024. A new hyper-heuristic based on adaptive simulated annealing and reinforcement learning for the capacitated electric vehicle routing problem. *Expert Systems with Applications* 252, 124197.
- Vaswani, A., Shazeer, N., Parmar, N., Uszkoreit, J., Jones, L., Gomez, A.N., Kaiser, L., Polosukhin, I., 2017. Attention is all you need, in: Advances in Neural Information Processing Systems.
- Vinyals, O., Fortunato, M., Jaitly, N., 2015. Pointer networks, in: Advances in Neural Information Processing Systems.
- Williams, R.J., 1992. Simple statistical gradient-following algorithms for connectionist reinforcement learning. *Machine Learning* 8, 229–256.
- Wu, Z., Pan, S., Chen, F., Long, G., Zhang, C., Yu, P.S., 2021. A comprehensive survey on graph neural networks. *IEEE Transactions on Neural Networks and Learning Systems* 32, 4–24.
- Xu, K., Hu, W., Leskovec, J., Jegelka, S., 2019. How powerful are graph neural networks?, in: International Conference on Learning Representations.
- Zhang, K., He, F., Zhang, Z., Lin, X., Li, M., 2020. Multi-vehicle routing problems with soft time windows: A multi-agent reinforcement learning approach. *Transportation Research Part C: Emerging Technologies* 121, 102861.
- Zhang, Z., Liu, H., Zhou, M., Wang, J., 2023. Solving dynamic traveling salesman problems with deep reinforcement learning. *IEEE Transactions on Neural Networks and Learning Systems* 34, 2119–2132.